

Development of Chromanes as Novel Inhibitors of the Uncoupling Proteins

Eduardo Rial,^{1,*} Leonor Rodríguez-Sánchez,¹ Patricio Aller,¹ Arancha Guisado,¹ M. Mar González-Barroso,¹ Eunáte Gallardo-Vara,¹ Mariano Redondo-Horcajo,¹ Esther Castellanos,² Roberto Fernández de la Pradilla,² and Alma Viso²

¹Centro de Investigaciones Biológicas—CSIC, 28040 Madrid, Spain

²Instituto de Química Orgánica General—CSIC, 28006 Madrid, Spain

*Correspondence: rial@cib.csic.es

DOI 10.1016/j.chembiol.2010.12.012

SUMMARY

The uncoupling proteins (UCPs) are mitochondrial carriers that modulate the energetic efficiency and, as a result, can lower superoxide levels. Here, we describe the discovery of a small-molecule inhibitor of the UCPs. Screening of potential UCP1 regulators led to the identification of chromane derivatives that inhibit its proton conductance. Members of the UCP family can act as a defense against oxidative stress and, thus, UCP2 plays a protective role in tumor cells. High UCP2 levels have been associated with chemoresistance. We demonstrate that chromanes also inhibit UCP2 and, in HT-29 human carcinoma cells, cause oxidative stress. The chromane derivatives can act synergistically with chemotherapeutic agents; for instance, they increase the toxicity of arsenic trioxide in HT-29 cells. These findings open a promising line in the development of novel anticancer agents.

INTRODUCTION

The uncoupling proteins (UCPs) are carriers that belong to the protein superfamily constituted by the metabolite transporters of the mitochondrial inner membrane. In mammals, five genes encode proteins considered UCPs (Ledesma et al., 2002a; Krauss et al., 2005). UCP1 is present in brown adipose tissue (BAT), UCP2 is ubiquitous, and UCP3 is expressed in heart, skeletal muscle, and brown adipose tissue. UCP4 and BMCP1 (UCP5) are predominantly expressed in the nervous system. Genes homologous to the mammalian UCPs have been described not only in most phyla of the animal kingdom but also in plants and unicellular eukaryotes (Ledesma et al., 2002a). The function of the different members of the UCP protein family is not fully established. Their biological activity appears to be linked to the modulation of the efficiency of the oxidative phosphorylation, although the actual molecular mechanism may vary among the different family members. This energy-dissipating mechanism is used in functions as diverse as the elimination of an excess calorie intake, regulation of insulin secretion, or maintenance of body temperature (Krauss et al., 2005). Because

the UCPs presumably increase the rate of mitochondrial respiration, an increase in their activity would also lead to a reduction in the mitochondrial production of superoxide. In fact, UCPs are up-regulated in many physiological situations where there is oxidative stress, and there are data showing that their overexpression reduces ROS damage. As a consequence, UCPs are widely considered as an additional element of antioxidant defense (Brand and Esteves, 2005; Nübel and Ricquier, 2006; Echtay, 2007; Baffy, 2010). Although the acceleration of respiration due to UCP-mediated uncoupling would lead to a reduction in ROS production, it has also been proposed that UCPs could induce a metabolic shift that would promote glycolysis and therefore indirectly lower ROS production (Bouillaud, 2009).

The mitochondrial activity of the UCPs is regulated by different ligands, although the physiological relevance of some of them is unclear. Only the physiological regulation of the uncoupling protein from BAT, UCP1, is well understood. Cytosolic purine nucleotides inhibit UCP1, while fatty acids override the inhibition and increase its proton conductance (Rial and González-Barroso, 2001). This regulatory mechanism fits precisely with its physiological context: noradrenaline binds to β -receptors, initiating a cAMP-dependent lipolytic cascade where the fatty acids liberated are the substrates that mitochondria will oxidize and the activators of UCP1 (Rial and González-Barroso, 2001). Although nucleotides and fatty acids are the more prominent regulators, there are other ligands that modulate the proton conductance in UCP1. Thus, *all-trans*-retinoic acid (ATRA) is a high-affinity activator of the protein (Rial et al., 1999) and, interestingly, also is a powerful transcriptional activator of the *ucp1* gene (Alvarez et al., 1995). Additionally, reduced ubiquinone lowers the affinity of UCP1 for nucleotides and, as a result, facilitates the activation by fatty acids (Swida-Barteczka et al., 2009). Ubiquinone also increases the affinity of UCP1 for ATRA (Tomás et al., 2002).

The regulation of the rest of the members of the UCP family is not yet understood (Brand and Esteves, 2005; Cannon et al., 2006; Echtay, 2007; Azzu and Brand, 2010). The interpretation of most data is complicated by the discovery that the adenine nucleotide translocator (ANT) could be responsible for some of the effects ascribed to the UCPs. Furthermore, the ANT has been shown to contribute significantly to the basal proton conductance (Brand et al., 2005). The inhibition of proton transport by GDP has often been used as diagnostic for the involvement of a UCP in the modulation of the efficiency of the oxidative phosphorylation, but GDP, although not translocated by the

ANT, does inhibit the proton conductance via ANT (Khailova et al., 2006). The involvement of the UCPs in the defense against oxidative stress led to the investigation of possible regulators that could be generated when ROS levels rise. Thus, superoxide and lipid peroxidation products such as hydroxynonenal have been proposed to activate the UCPs (Echtay et al., 2002, 2003). These peroxidation products would set off a negative feedback mechanism by which the activation of the UCPs would increase respiration, lower ROS production, and thereby protect against oxidative stress. Although this hypothesis is very attractive, the activation by ROS-derived products has not been confirmed by some laboratories, and, as previously stated, the ANT could account for the ROS-induced changes in proton conductance (Couplan et al., 2002; Shabalina et al., 2010).

The development of specific inhibitors of the UCPs would greatly facilitate the investigation of their transport activity and regulation. Here we describe the identification and synthesis of a family of inhibitors of the uncoupling proteins. We demonstrate that certain chromane derivatives inhibit the fatty acid-induced proton conductance of UCP1 without affecting other components of the oxidative phosphorylation (OXPHOS) system. Furthermore, the chromane derivatives also inhibit UCP2 in yeast mitochondria. Finally, we show that in HT-29 tumor cells, which express UCP2, chromanes inhibit respiration and increase ROS levels. Interestingly, the inhibitor lowers the viability of HT-29 cells, increasing the efficacy of antitumor drugs that cause oxidative stress, such as arsenic trioxide or doxorubicin.

RESULTS AND DISCUSSION

Chromane Derivatives Inhibit the Uncoupling Protein UCP1

All-trans retinoic acid (ATRA) up-regulates the expression of the uncoupling proteins UCP1 and UCP2 (Alvarez et al., 1995; Hatakeyama and Scarpace, 2001). We have previously shown that ATRA also activates the proton conductance of UCP1 and UCP2 (Rial et al., 1999). Because a large collection of compounds structurally related to ATRA has been synthesized as specific ligands for retinoid receptors (Altucci et al., 2007), we screened a set of retinoids to get an insight into the specificity of the UCP1 ligand (Tomás et al., 2004). The screening protocol was based on the analysis of the effect of the compounds on the rate of NADH oxidation by mitochondria isolated from *Saccharomyces cerevisiae* that expressed UCP1 (Tomás et al., 2004). Under our experimental conditions, in the absence of added regulators, yeast mitochondria expressing UCP1 present a respiratory activity higher than that of control mitochondria (Figure 1A). This higher respiration rate can be inhibited by purine nucleotides and represents the basal proton conductance of UCP1 (González-Barroso et al., 1998; Jiménez-Jiménez et al., 2006).

Figure 1A shows the effect of ATRA in control mitochondria and mitochondria containing UCP1. The low concentrations of ATRA used only stimulate respiration (NADH oxidation) when UCP1 is present. We have previously shown that the increase can be inhibited by GDP (Rial et al., 1999; Tomás et al., 2004). We have also described that other retinoids, which must possess a free carboxylate group, are also activators of UCP1. Interestingly, the retinoid AGN199108 displayed a nonspecific stimulation

of NADH oxidation in control mitochondria (Figure 1B), an uncoupling effect that was also evident in UCP1-containing mitochondria. However, at low concentrations, this retinoid decreased the NADH oxidation rate in UCP1 mitochondria, thus suggesting the inhibition of the basal proton conductance of UCP1. The reason behind this mixed behavior could be the ester hydrolysis under aqueous conditions that generates two new organic acids, 2,2,4,4-tetramethylchroman-6-carboxylic acid and (E)-3-(4-hydroxyphenyl)acrylic acid, from the starting retinoid. Because small organic acids can permeate across the lipid bilayer, the two resulting compounds could act as protonophores and thus explain the observed nonspecific uncoupling activity.

Nucleotides inhibit UCP1 by binding deep inside the α -helical bundle core with the purine ring interacting with the matrix loops (González-Barroso et al., 1999; Ledesma et al., 2002b). The chromane moiety of the retinoid AGN199108 could act as a surrogate of the purine ring, and we thus hypothesized that this moiety would be responsible for the inhibition. To test the hypothesis, two chromane derivatives, 6-bromo-8-isopropyl-2,2-dimethylchromane (CSIC-E183) and 8-isopropyl-2,2-dimethylchroman-6-carboxylic acid (CSIC-E137), were synthesized and their activity tested. The chromane CSIC-E137 retained the carboxylic moiety, whereas in the chromane CSIC-E183, the position C-6 at the chromane ring was substituted by a bromine to remove the protonable residue. Experiments with control mitochondria confirmed the essential role of the carboxylate for the protonophoric properties because the bromine-substituted compound had no significant effect on respiration (Figure 1C). The inhibitory properties of CSIC-E183 on UCP1 containing mitochondria were tested in the presence of palmitate to include a physiological activator. Data clearly demonstrate that CSIC-E183 was able to inhibit both the palmitate-induced and the basal proton conductance of UCP1 because the rate of NADH oxidation was decreased to the level of control mitochondria (Figure 1D).

Characterization of the Active Compounds

To determine the structural requirements of the inhibitory compounds, we designed and synthesized a series of chromane derivatives of general structure I, and some of them proved to be valuable inhibitors of UCP1. In these derivatives, we analyzed the effect of the substituents in four different positions (R^1 – R^4) thus allowing us to establish the first basis of their influence on the inhibitory activity of these chromanes. Table 1 gathers the new series of compounds examined and presents the data obtained when tested in control yeast mitochondria and mitochondria containing UCP1. The EC_{50} was calculated from the difference in inhibition kinetics (see Figures S1 and S2 available online).

One of the most marked structural features for inhibition of UCP1, which arises upon inspection of Table 1, is the crucial presence of a substituent at C-8 of the chromane skeleton. Thus, lower EC_{50} values are obtained when R^4 is an alkyl group than when R^4 is a proton (entries 1–9 vs. entries 12–15). Linear and branched alkyl groups are well-tolerated at the C-8 position increasing the potency of the inhibitors, mainly for the ethyl group (entries 1–4); however, a methyl ketone at this position precludes the inhibition (entry 10). We also evaluated the influence of the nature of the group R^3 . The presence of an acidic

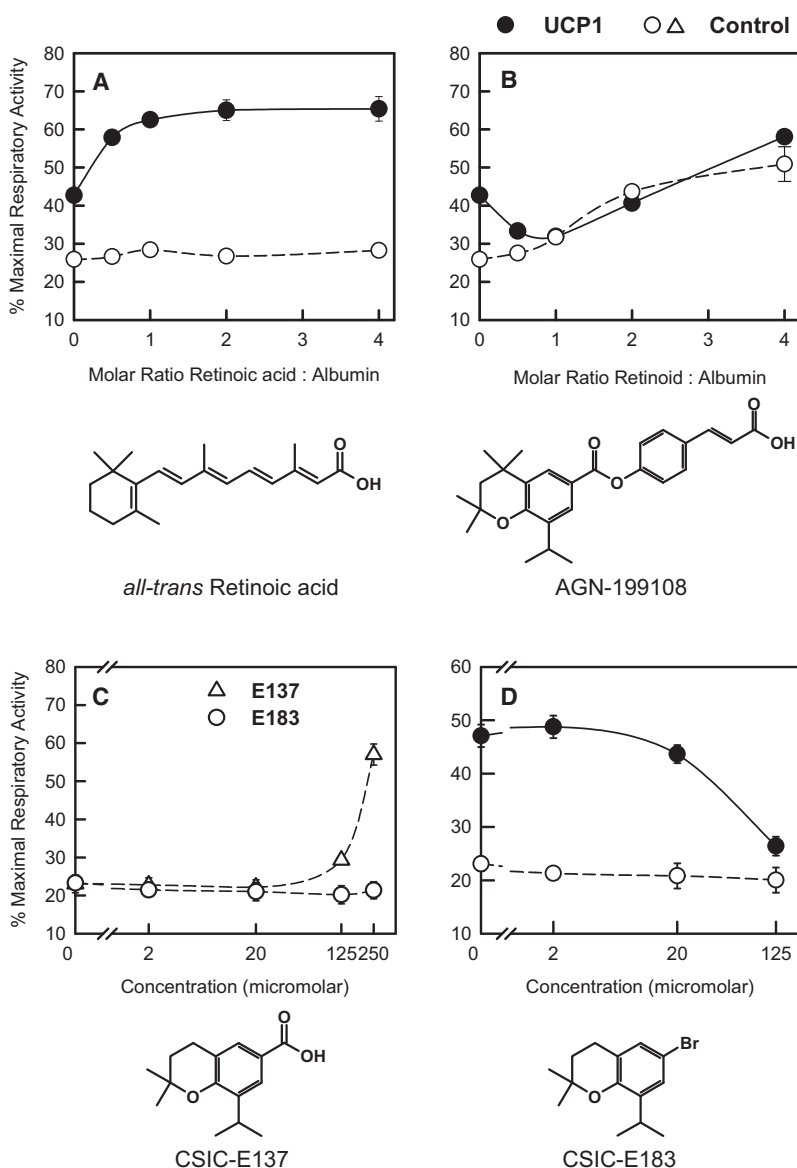


Figure 1. Chromane Derivatives Inhibit the Proton Conductance of UCP1

The activity of UCP1 is determined from the rate of NADH oxidation of mitochondria from yeast that express UCP1 recombinantly (filled circles) and compared with control yeast mitochondria (empty circles). Rates of respiration are expressed as a percentage of the maximal rate of respiration that is determined in the presence of 1 μ M FCCP. Data are means \pm SEM of 4–6 independent experiments each performed in triplicate.

(A) Activation of respiration in UCP1 containing mitochondria by ATRA and lack of effect on control mitochondria.

(B) Activation by the retinoid AGN-199108.

(C) Effect of the chromanes CSIC-E137 and CSIC-E183 on control yeast mitochondria.

(D) Effect of the compound CSIC-E183 on control yeast mitochondria and UCP1-containing yeast mitochondria.

CSIC-E379 (8-isopropyl-2,2-dimethyl-6-phenylchromane; EC_{50} , 20 μ M), was used as inhibitor for the remaining of the work. Similarly, the chromane CSIC-E167 was subsequently used as inactive control because of its lack of effect on UCP1.

Chromane Derivatives Inhibit the Uncoupling Protein UCP2

We have previously reported that, when the uncoupling protein UCP2 is expressed recombinantly in *S. cerevisiae*, the isolated mitochondria present a higher state 4, whereas the phosphorylation rate or the maximal respiratory activity remain unchanged (Rial et al., 1999). The effect of the chromanes on UCP2 was also tested using the NADH-based screening protocol. Under these experimental conditions, UCP2-containing mitochondria presented a higher basal respiratory activity, although the difference with control mitochondria accounted for only 9% of the maximal respiratory capacity (Figure 2; Figure S3). The active chromane CSIC-E379 caused the inhibition of the UCP2-dependent respiratory activity that was evident

when the nonspecific effects on control mitochondria were taken into account (Figure 2). The estimated EC_{50} was close to 30 μ M and thus similar to the one obtained with UCP1 (Table 1). As expected, when the UCP1-inactive compound CSIC-E167 was tested on mitochondria containing UCP2, the NADH oxidation rate was not modified (Figure 2; Figure S3).

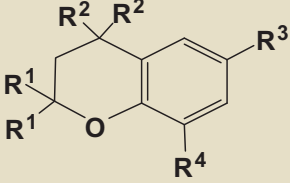
moiety deprives the compound of any inhibitory capacity (EC_{50} , >200 μ M) that is recovered, however, upon esterification (EC_{50} , 27 μ M) (entries 16 vs. 6). The absence of a substituent (R^3 = H) and the substitution by a bromine allow for moderate inhibitory activities (entries 9 and 3). Alternatively, the introduction of an aromatic group (R^3 = Ph) leads to the most potent inhibitor in the series (entry 5); in contrast, a vinyl group in this position hampers the inhibitory activity (entry 11). Finally, we examined the nature of the substitution at the oxygenated ring, and no significant differences have been found between the chromane skeletons examined, 2,2-dialkylated and 4,4-dialkylated (R^1 = Me vs. R^2 = Me, entries 6/7 and 8/9); however, the need for the chromane ring has been proven with the lack of inhibition of CSIC-E243 (4-bromo-2-isopropyl-1-methoxybenzene), a monocyclic analog to CSIC-E183 and CSIC-E179 (entries 17, 3, and 8). Consequently, the chromane with the highest affinity,

when the nonspecific effects on control mitochondria were taken into account (Figure 2). The estimated EC_{50} was close to 30 μ M and thus similar to the one obtained with UCP1 (Table 1). As expected, when the UCP1-inactive compound CSIC-E167 was tested on mitochondria containing UCP2, the NADH oxidation rate was not modified (Figure 2; Figure S3).

Chromane Do Not Affect OXPHOS in Liver Mitochondria

The screening protocol used to characterize the inhibitory properties of the chromane derivatives is performed under nonphosphorylating conditions. Because we had hypothesized that the inhibition of the proton transport activity of UCP1 by chromane moiety was likely due to its resemblance with the purine ring, it was necessary to assess whether the chromane derivatives were interfering with the exchange of ADP/ATP or the phosphorylation of ADP at the F_0F_1 -ATPase. Figure 3 presents the effect of the

Table 1. Chemical Structure, Nomenclature, and Activity of the Chromane Derivatives Synthesized and Characterized in the Present Study

Entry	Compound					EC ₅₀ (μM)
		R ¹	R ²	R ³	R ⁴	
1	CSIC-E225	Me	H	Br	Et	34
2	CSIC-E221	Me	H	Br	Pr	54
3	CSIC-E183	Me	H	Br	i-Pr	111
4	CSIC-E231	Me	H	Br	t-Bu	39
5	CSIC-E379	Me	H	Ph	i-Pr	20
6	CSIC-E1127	Me	H	CO ₂ Et	i-Pr	27
7	CSIC-E1131B	H	Me	CO ₂ Et	i-Pr	32
8	CSIC-E179	H	Me	Br	i-Pr	132
9	CSIC-E155	Me	H	H	i-Pr	98
10	CSIC-E161	H	Me	Br	COCH ₃	>200
11	CSIC-E393	Me	H	CH=CH ₂	i-Pr	>200
12	CSIC-E1125	Me	H	CO ₂ Et	H	135
13	CSIC-E375	Me	H	Ph	H	109
14	CSIC-E167	Me	H	Br	H	>200
15	CSIC-E1113	H	Me	CO ₂ Et	H	>200
16	CSIC-E137	Me	H	CO ₂ H	i-Pr	>200
17	CSIC-E243	4-bromo-2-isopropyl-1-methoxybenzene (see text)				>250

The concentration that causes a 50% inhibition of transport activity of UCP1 (EC₅₀) was calculated from the difference between the NADH oxidation rates in UCP1-containing mitochondria and control mitochondria. Experimental data for each compound are included in [Figures S1 and S2](#).

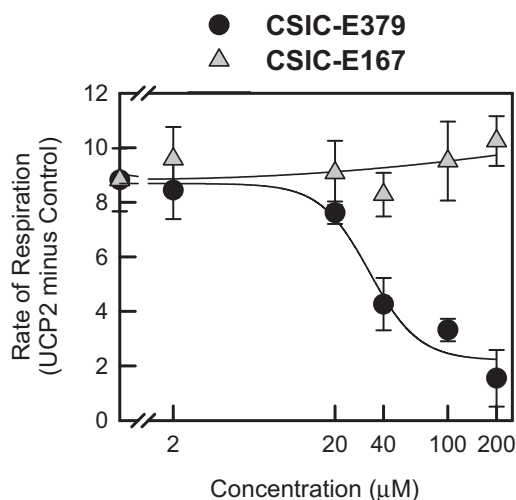


Figure 2. Chromane Derivatives Inhibit Respiration in UCP2-Containing Yeast Mitochondria

Respiration was determined from the rate of NADH oxidation in control mitochondria and mitochondria isolated from yeasts expressing UCP2 recombinantly, either in the presence of CSIC-E379 (circles) or CSIC-E167 (triangles). Data are expressed as the difference in the NADH oxidation rate of UCP2 minus control mitochondria (see also Figure S3). Data points are means \pm SEM of 3 independent experiments each performed in triplicate.

chromane CSIC-E379 on rat liver mitochondria. The compound CSIC-E379 had no effect on the basal respiratory rate (state 4), thus ruling out a direct effect on the respiratory complexes or the membrane permeability. Although this chromane had no statistically significant effect on the phosphorylation of added ADP (state 3), a trend is apparent showing a 10% inhibition when the concentration was raised to 60 μ M. Therefore, the chromane CSIC-E379 does not significantly affect the OXPHOS system.

Chromane Derivatives Inhibit the Cellular Respiration of the Cancer Cell Line HT-29

The biochemical activity of the UCPs is to lower the efficiency of the oxidative phosphorylation, presumably by increasing the membrane proton conductance. This mild uncoupling would lead to an increase in respiration, which results in a lower generation of superoxide due to the decrease in proton-motive force. This uncoupling effect could constitute a mechanism of defense against oxidative stress. Indeed, UCPs are up-regulated in physiological situations where there is oxidative stress and, furthermore, their overexpression reduces ROS damage (Echtay, 2007; Azzu and Brand, 2010; Baffy, 2010; Rial et al., 2010).

The effect of the chromane CSIC-E379 on the cellular respiration was investigated using the cell line HT-29, a colon cancer cell line that expresses the uncoupling protein UCP2 (Figure S4). Cells were incubated for 1 hr in the presence of the chromane, and then the respiratory activity was determined on an XF24 Extracellular Flux Analyzer. Figure 4A shows that the chromane causes a 22% decrease in the basal rate of respiration, in agreement with the data obtained with UCP2-containing yeast mitochondria. Genipin, an iridoid glucoside, has also been described to inhibit UCP2. Genipin is extracted from the fruits of *Gardenia jasminoides* and is used in traditional Chinese medicine to treat,

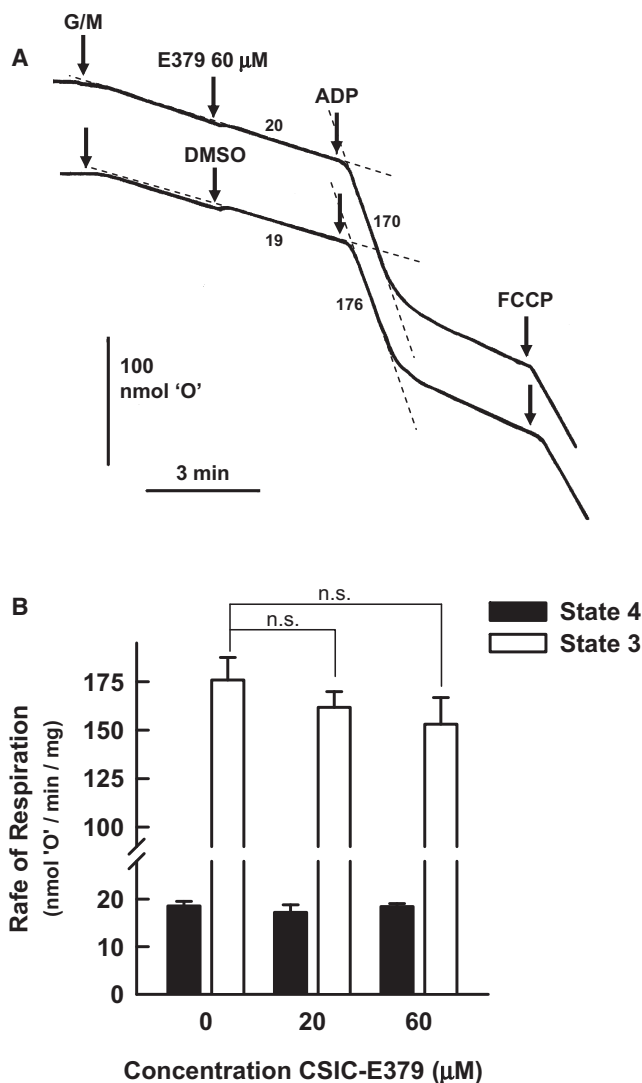


Figure 3. Effect of the Chromane CSIC-E379 on the Oxidative Phosphorylation of Isolated Rat Liver Mitochondria

(A) Representative traces with the measurement of the oxygen consumption in the presence and absence of the compound CSIC-E379. Respiration was initiated with the addition of glutamate 5 mM plus malate 5 mM (G/M); the state 3 respiration rate was determined after the addition of ADP 0.2 mM. FCCP 1 μ M was added at the end of the run. Rates are expressed as nmol "O" per minute and milligrams of protein.

(B) Effect of CSIC-E379 on the rate of respiration in the basal state 4 (filled bars) and in state 3 (empty bars). Bars represent the mean \pm SEM of 4–5 independent experiments. There are no significance differences (n.s.) between the rates in the presence and absence of the chromane.

among other diseases, type 2 diabetes. Zhang et al. (2006) reported that genipin inhibited UCP2 in β -cells, raising ATP levels and increasing insulin secretion while reducing insulin-stimulated glucose uptake in 3T3-L1 adipocytes (Zhou et al., 2009). Mailloux et al. (2010) have recently reported that genipin also inhibits respiration in UCP2 overexpressing leukemia cells.

Bouillaud (2009) has proposed a "metabolic hypothesis," whereby UCP2 (and UCP3) has a transport activity that does not involve proton translocation. The working model proposes

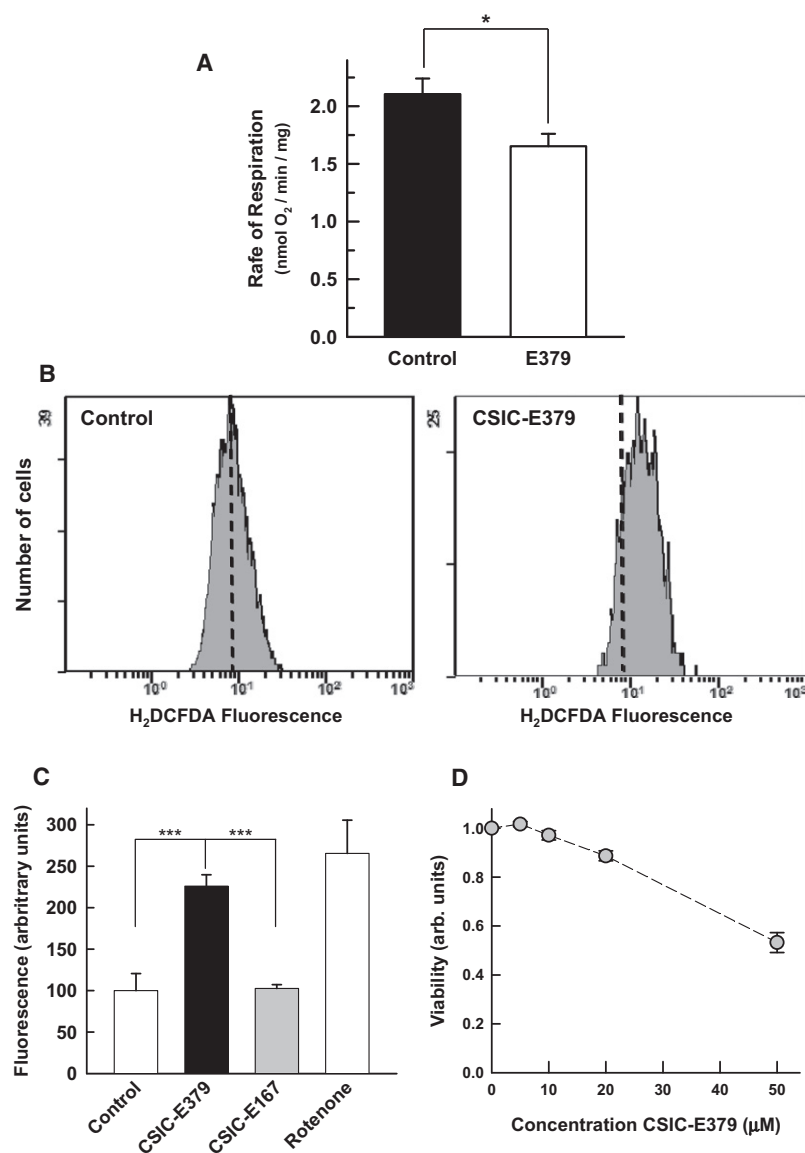


Figure 4. The chromane CSIC-E379 inhibits mitochondrial respiration in HT-29 colon cancer cells causing oxidative stress and decreasing their viability

(A) Basal rate of oxygen consumption of HT-29 cells after subtraction of the rate obtained in the presence of antimycin A and rotenone. Cells were incubated for 1 hr in the presence (empty bar) or in the absence (filled bar) of 20 μM CSIC-E379. Data are the mean ± SEM of three independent experiments.

(B) Representative flow-cytometry histograms of the ROS levels determined with the fluorescent probe H₂DCFDA in control HT-29 cells (left panel) or cells treated for 24 hr with CSIC-E379.

(C) Histograms summarizing the effect of the chromanes CSIC-E379 and CSIC-E167 on ROS levels in HT-29 cells after a treatment for 24 hr. Treatment with the respiration inhibitor rotenone for 1 hr is used as positive control for ROS generation. Bars represent the mean ± SEM of 5–6 independent experiments.

(D) Effect of the compound CSIC-E379 on the viability of HT-29 cells after a 24 hr treatment determined from the rate of reduction of the reagent WST-1. Data points represent the mean ± SEM of 8–10 independent experiments each performed in triplicate.

See also Figure S4.

that UCP2/3 would catalyze the export of pyruvate from the matrix, thus limiting substrate supply to mitochondria, and that would also lead to a metabolic shift that would promote glycolysis. The lower redox pressure on the mitochondrial respiratory chain would indirectly lead to a decreased ROS production. The observed effects of genipin or the chromane derivatives would not be compatible with this hypothetical transport activity because the predicted effect of the inhibition of UCP2 would have been a higher (or an unchanged) rate of respiration. The inconsistency is even more evident when the effect of the chromanes on UCP2-containing yeast mitochondria is taken into consideration.

Chromane Derivatives Increase the Production of Superoxide and Decrease the Viability of the Cancer Cell Line HT-29

Compared with their nontransformed counterparts, cancer cells often present high intrinsic oxidative stress, which is probably

a determinant for oncogenic transformation (Trachootham et al., 2009). Cells adapt to increased ROS levels with defense mechanisms that include the up-regulation of antioxidant enzymes (superoxide dismutase, catalase, and glutathione peroxidase) and enzymes that regenerate nonenzymatic antioxidants, such as glutathione reductase or the thioredoxin system. In addition, tumor cells defend themselves against the deleterious effects of oxidative stress by promoting the expression of cell-survival proteins, such as Bcl-2, or by activating survival pathways such as PI3K/Akt or MEK/ERK (Trachootham et al., 2009; Pani et al., 2010). In this regard, UCP2 has been shown to be expressed in cancer cells (Carretero et al.,

1998; Harper et al., 2002; Horimoto et al., 2004; Samudio et al., 2008; Santandreu et al., 2009, 2010; Mailloux et al., 2010; Sastre-Serra et al., 2010; Baffy, 2010), and it has been proposed that UCP2 could be a metabolic strategy used by the tumor cells to develop resistance against radio- or chemotherapy (Harper et al., 2002; Mailloux et al., 2010; Baffy, 2010).

The capacity of the chromane derivatives to inhibit UCP2 and influence cell viability was first tested by analyzing their effect on ROS levels in HT-29 cells. Figure 4B presents representative histograms of ROS levels determined with fluorescent probe H₂DCFDA in control cells and cells treated for 24 hr with the chromane CSIC-E379. Data show that the active chromane CSIC-E379 causes an increase in ROS levels, similar to that obtained with rotenone, which is not evoked by the inactive compound CSIC-E167 used as a control (Figure 4C). The observed chromane-induced increase in ROS resembles those reported when tumor cells are treated with genipin (Mailloux

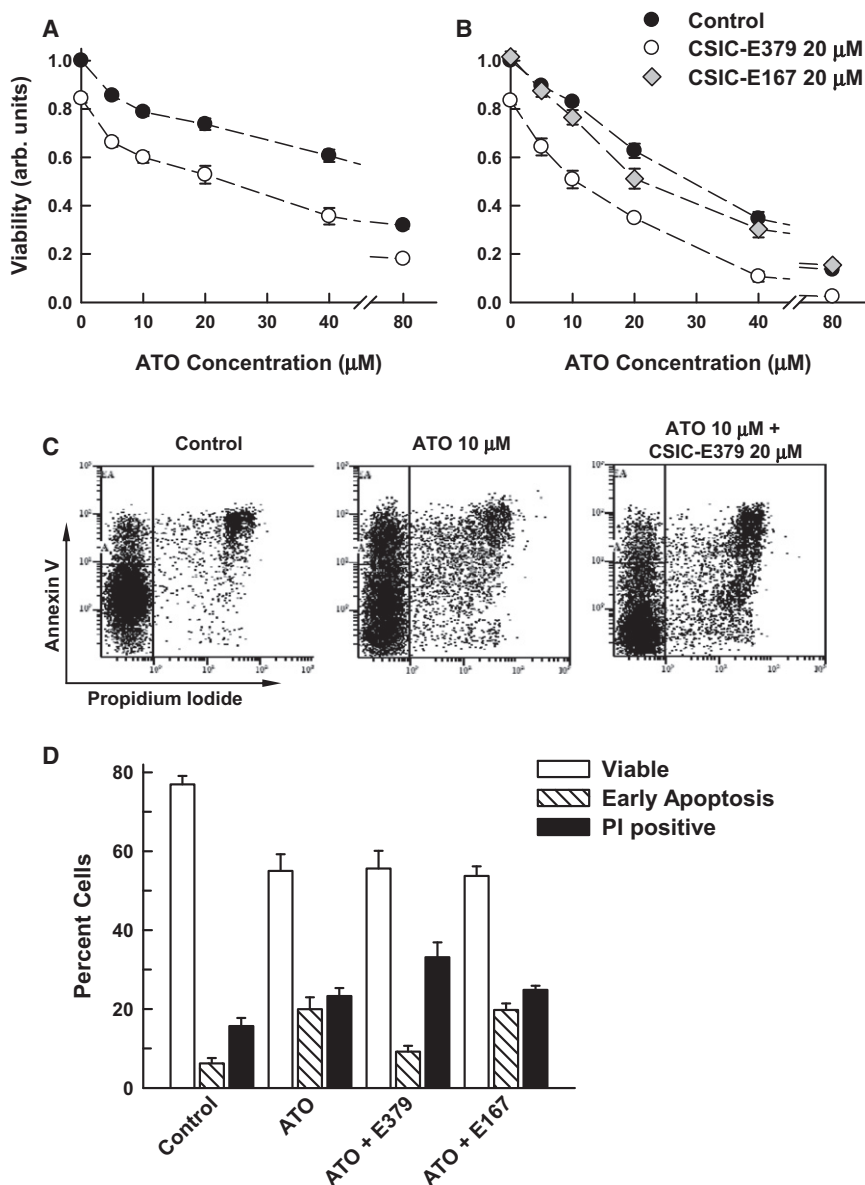


Figure 5. The compound CSIC-E379 sensitizes the cancer cell line HT-29 to arsenic trioxide

(A) Titration of the effect of ATO on the viability of the cells treated for 24 hr in the absence (filled circles) or in the presence of 20 μ M CSIC-E379 (empty circles).

(B) Effect of ATO on the viability of the cells treated for 48 hr in the absence of chromanes (filled circles), in the presence of 20 μ M CSIC-E379 (empty circles), or in the presence of 20 μ M CSIC-E167 (gray diamonds). In panels (A) and (B), data points represent the mean \pm SEM of 8–16 independent experiments each performed in triplicate. Difference between control values and those from CSIC-E379 treated cells are significant, with $p < 0.001$.

(C) Representative flow cytometry profiles of the effect of ATO and CSIC-E379 on HT-29 cells. Cells were treated for 24 hr, stained with Annexin-V and PI, and apoptosis subsequently was analyzed by flow cytometry. Left panel, control cells; central panel, cells treated with 10 μ M ATO; right panel, cells treated with 10 μ M ATO plus 20 μ M CSIC-E379.

(D) Histogram summarizing the analysis of the effect of the chromane derivatives CSIC-E379 and CSIC-E167 on the apoptosis of HT-29 cells. Empty bars represent the viable cells and are those that are not stained with Annexin-V or PI; hatched bars represent the cells in the early apoptotic phase that are Annexin-V positive and PI negative; and black bars represent the cells in late apoptosis plus necrotic cells and therefore include all PI positive cells. Bars represent the mean \pm SEM of 3–8 independent experiments each performed in duplicate.

Chromane Derivatives Potentiate the Efficacy of the Cytotoxic Drug Arsenic Trioxide

As indicated above, the elevated intrinsic oxidative stress of tumor cells is behind the efficacy of therapies with some anti-tumor drugs or radiation. The increase in oxidative stress can be due to a direct

et al., 2010; Santandreu et al., 2010). It is worth recalling that the overexpression of UCP2 in the colon cancer cell line HCT116 has been shown to decrease the ROS levels (Derdak et al., 2008).

The intrinsic elevated level of oxidative stress makes tumor cells more susceptible to the action of ROS-inducing cytotoxic agents, a property that has been satisfactorily exploited in anti-tumor therapies (Lau et al., 2008; Trachootham et al., 2009). We therefore tested the effect of the chromane CSIC-E379 on the cell viability and observed that the concentration (20 μ M) and treatment time (24 hr) that were shown to increase the ROS level caused a moderate, although significant, decrease in viability (Figure 4D). When the concentration of CSIC-E379 was raised to 50 μ M, the decrease in viability was close to 50%. Again, genipin has also been shown to reduce the viability of other tumor cells lines that express UCP2 (Mailloux et al., 2010; Santandreu et al., 2010).

generation of ROS and/or to an interference with the antioxidant defenses. Arsenical compounds, such as arsenic trioxide (ATO), have been shown to be effective in the treatment of acute promyelocytic leukemia and other human cancers (Lau et al., 2008). Generation of ROS is one of the mechanisms explaining the induction of apoptosis by ATO. Interestingly, the ATO efficacy is determined, at least in part, by the intracellular redox status. Thus, it is known that its cytotoxicity is greatly dependent on the intracellular content of reduced glutathione and that, for example, depletion of glutathione stores sensitizes cells to ATO (Yi et al., 2002; Lau et al., 2008). In the same context, we have recently shown that genistein, a soy-derived isoflavone, behaves as a pro-oxidant agent potentiating ATO-induced apoptosis in human leukemia cells via ROS overproduction and the activation of the ROS-inducible protein kinases p38-MAPK and AMPK (Sánchez et al., 2008).

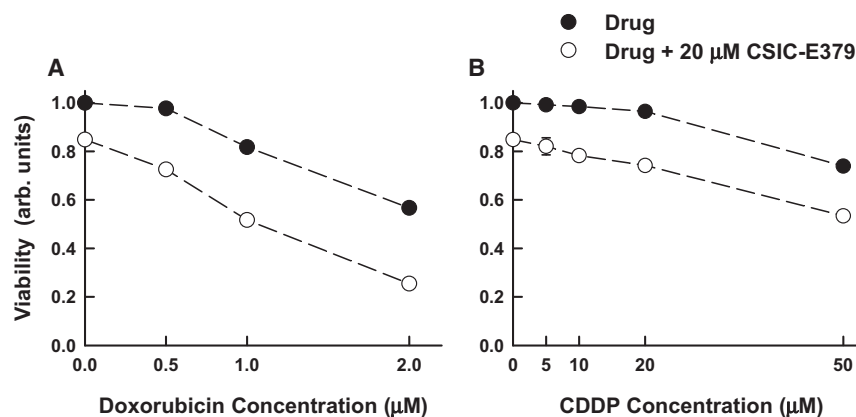


Figure 6. The chromane derivative CSIC-E379 sensitizes HT-29 cancer cells to doxorubicin and cisplatin

Cell viability was determined from the reduction of WST-1. In the two panels, data points represent the mean \pm SEM of at least 9 independent experiments each performed in triplicate. The difference between the control values and those from CSIC-E379 treated cells are significant, with $p < 0.001$. (A) Effect of doxorubicin on the viability of the cells treated for 48 hr in the absence (filled circles) or in the presence of 20 μ M CSIC-E379 (empty circles). (B) Effect of CDDP on the viability of the cells treated for 48 hr in the absence (filled circles) or in the presence of 20 μ M CSIC-E379 (empty circles).

Because we have shown that the chromane CSIC-E379 increases ROS levels in the cancer cell line HT-29, it was of interest to determine whether its combination with ATO could also potentiate the effect of the antitumor drug. Figure 5A presents the effect of increasing ATO concentrations on the viability of HT-29 cells incubated for 24 hr either in the absence or in the presence of 20 μ M CSIC-E379. Data revealed that the decreased in viability was markedly pronounced in the presence of the UCP2 inhibitor but the effect appeared as additive. However, when the treatments were maintained for 48 hr (Figure 5B), the ATO toxicity was clearly potentiated, being more evident at very low doses. Thus, 5 μ M ATO (concentration close to the useful therapeutic dose) caused a 10% reduction in viability, whereas in the presence of CSIC-E379, the reduction was close to 35%. As expected, the inactive chromane CSIC-E167 had no potentiating effect.

The cell viability is often inferred from the metabolic activity and, thus, we used a protocol based on the reduction of the reagent WST-1 that is dependent on the rate of NAD(P)H formation. To ascertain the effect of the chromanes on cell death, we analyzed the cellular apoptosis and necrosis using annexin-V labeling combined with propidium iodide (PI) staining. Figure 5D summarizes the results that revealed that, as expected, 10 μ M ATO decreases the number of viable cells and causes a marked increase in annexin-V-positive cells that represent cells in the early apoptotic phase. When the inhibitor was present, the reduction in viable cells was not significantly different, but the number of PI-positive cells (late apoptotic or necrotic cells) was greatly increased. It appears that UCP2 inhibition exacerbates cell death.

The potentiating effect of the chromane CSIC-E379 was also tested with the antitumor drugs cisplatin (CDDP) and doxorubicin. The two drugs are known to induce oxidative stress, and previous studies have shown that UCP2 could influence their toxicity (Derdak et al., 2008; Mailloux et al., 2010; Santandreu et al., 2010). Figure 6 presents the effect of CSIC-E379 on the viability after the treatment for 48 hr with varying concentrations of the two drugs. The inhibitor cooperates in more than additive manner with the two agents, thus confirming that UCP2 inhibition sensitizes cancer cells to agents commonly used in chemotherapy.

Conclusion

The 3D-structure of the UCPs is not available, but the structure of the ANT has revealed the common structural scaffold of the

mitochondrial carriers (Nury et al., 2006). The basic fold is a barrel formed by the six transmembrane α helices that is closed at the matrix side. The α helices define a hydrophilic cavity opened to the intermembrane space and that enters deeply into the protein, constituting the translocation pathway. The nucleotide-binding site in UCP1 is probably the best-known structural feature of the protein. Photoaffinity labeling and site-directed mutagenesis experiments have shown that the nucleotide enters the protein through its cytosolic side and gets deep inside the cavity to interact with the loops at the bottom of the barrel. We have proposed that the purine ring would fit in a hydrophobic pocket and that its stabilization would occur through stacking interactions, as it happens in other nucleotide binding proteins (González-Barroso et al., 1999; Ledesma et al., 2002b). The hydrophobicity and planar structure of the chromane derivatives identified in the present report suggest that the chromane could probably occupy the same site than the purine ring.

As we have previously stated, GDP inhibition of the mitochondrial proton conductance was considered for many years as diagnostic of the involvement of a UCP. However, it has become clear that the activity of the ANT, being the most abundant carrier, overlaps with that of the UCPs and can also be inhibited by GDP. As a result, doubts have been shaded on some biological activities attributed to the UCPs. The discovery that the effect of genipin in β -cells is mediated by UCP2 has led to its use as a "specific" UCP2 inhibitor. However, genipin is a natural product used in traditional Chinese medicine to treat a variety of diseases. Thus, it exhibits anti-inflammatory and anti-angiogenic activities, inhibits lipid peroxidation, and suppresses cell proliferation and migration (Koo et al., 2004; Yamazaki and Chiba, 2008; Kim et al., 2010). Recent studies have also reported that genipin protects against D-galactosamine/lipopolysaccharide-induced hepatic apoptosis and liver failure by preventing oxidative stress, apoptosis, NF- κ B nuclear translocation, and nuclear c-Jun expression (Kim et al., 2010). Finally, it should be borne in mind that genipin is a highly reactive nonspecific cross-linking agent that, for example, is used to generate biocompatible polymers (Slusarewicz et al., 2010). Therefore, the possible side effects imply that caution should be exerted when using genipin as a "specific" UCP2 inhibitor. The above facts evidence the need for new and selective inhibitors of the uncoupling proteins. Further optimization of the chromane derivatives

described here should lead to a new generation of such high-affinity inhibitors. Data presented point to their application as tools for uncoupling protein research and even as new chemotherapeutic agents.

SIGNIFICANCE

Mitochondria play a key role in cellular processes that range from energy production to redox or calcium homeostasis, participating in a wide range of metabolic pathways. However, although mitochondria are essential for cell survival, a variety of death signals converge on mitochondria making this organelle also central to cell death. Mitochondria are also one of the main sites of ROS production, and thus mechanisms that prevent ROS damage are not only critical for the preservation of their function but also for cell survival. The uncoupling proteins (UCPs) control the energetic efficiency, and one of the consequences is that they participate in the control of mitochondrial ROS production.

The search for new regulators of the uncoupling activity of UCP1 has led to the discovery of a small-molecule inhibitor of the UCPs that we have presented. UCP2 appears as one of the most interesting pharmacological targets of the chromane derivatives, and, thus, we have explored the application of the inhibitor to increase oxidative stress in tumor cells with the aim of generating an imbalance in ROS status and thus make the cells more susceptible to other chemotherapeutic drugs. The use of selective combinations of drugs to enhance their therapeutic efficacy is a common approach undertaken in cancer treatment. Because UCP2 appears to be linked to the antioxidant defense of tumor cells and has even been shown to promote chemoresistance (Harper et al., 2002; Derdak et al., 2008; Mailloux et al., 2010; Baffy, 2010), the development of small-molecule UCP2 inhibitors is a promising new step in the development of novel anticancer strategies.

EXPERIMENTAL PROCEDURES

Synthesis of Chromane Derivatives

The syntheses of 4-bromo-2-isopropyl-1-methoxybenzene (Burnel and Caron, 1992), 6-bromo-2,2-dimethylchromane (Bernard et al., 1998), ethyl 2,2-dimethylchroman-6-carboxylate (Teng et al., 1997), and 6-phenyl-2,2-dimethylchromane (Ishino et al., 2001) were previously reported. 2,2-Dimethylchromanes were prepared by cyclization of phenols with 3-methyl-2-buten-1-ol (Ishino et al., 2001). 4,4-Dimethyl chromanes were prepared by a sequence that entails *O*-alkylation of phenols with 4-bromo-2-methyl-2-butene, acetoxymercuration/reduction, and cyclization mediated by AlCl_3 (Janusz et al., 1998). 6-Phenyl and 6-vinyl chromanes were prepared by a Stille coupling from 6-bromo chromanes and vinyl or phenyl tributylstannanes (McKean et al., 1987). 6-Carboxyethyl chromanes were obtained from 6-bromo chromanes with *t*-BuLi and ethyl chloroformate. Further saponification with NaOH yielded the carboxylic acid. Finally, 8-acetyl chromane was prepared from the chromane via Friedel-Crafts acylation with acetyl chloride and AlCl_3 . All the compounds were purified and characterized prior to submission to biological essays (see details in Supplemental Experimental Procedures).

Yeast Strains, Isolation of Yeast Mitochondria, and Determination of Mitochondrial NADH Oxidation

The procedures for recombinant expression of the rat uncoupling protein UCP1 or the mouse UCP2 in the *S. cerevisiae* strain W303 and the protocol

for the isolation of mitochondria from yeasts have been described previously (Arechaga et al., 1993). The control strain contained the same vector but with the UCP1 cDNA in the inverse orientation.

The rate of yeast mitochondrial respiration was determined from the decrease in NADH fluorescence as previously described (Tomás et al., 2004). Mitochondria (0.1 mg protein/ml) were incubated at 20°C in medium containing 0.65 M mannitol, 0.5 mM EGTA, 10 mM phosphate, 2 mM MgCl_2 , 3 μM essentially fatty-acid-free albumin, and 10 mM Tris/maleate (pH 6.8). When required, the medium also contained 9 μM palmitate (3:1 molar ratio to albumin). Respiration was initiated by the addition of 0.3 mM NADH. Experiments were performed on standard 96-well microtiter plates, and fluorescence was measured in a POLARstar Galaxy reader (BMG Labtechnologies). Excitation was set at 340 nm and emission at 470 nm.

Isolation of Liver Mitochondria and Determination of Respiration Rates

Mitochondria from rat liver were isolated as previously described (Heaton and Nicholls, 1976). Final pellet was resuspended in a buffer containing 250 mM sucrose, 5 mg/ml albumin, and 10 mM Tes (pH 7.4). Protein concentration was determined by the BCA method. The respiration experiments were carried out at 25°C in a Hansa-Tech oxygen electrode. Mitochondria (0.5 mg/ml) were suspended in medium containing 75 mM NaCl, 10 mM Tes, 1 mM EGTA, 1 mg/ml albumin, and 2 mM sodium phosphate (pH 7.0). Substrate was 5 mM glutamate plus 5 mM malate.

Cell Line and Measurements of Cellular Respiration

HT-29 colon carcinoma cells were obtained from the American Type Culture Collection. Cells were cultured at 37°C in a humidified 5% CO_2 atmosphere in DMEM (GIBCO) supplemented with 10% heat-inactivated FBS (Sigma), 2 mM L-glutamine, and 100 U/ml of penicillin/streptomycin (Invitrogen).

An XF24 Seahorse Bioscience instrument was used to measure the rate of oxygen consumption of HT-29 cells; 60,000 cells per well were seeded in XF24 cell culture plates in complete DMEM growth media and incubated at 37°C, 5% CO_2 for 24 hr prior to beginning the assay. For the XF24 assay, DMEM growth media was replaced by unbuffered DMEM supplemented with 25 mM glucose, 1 mM pyruvate, 2 mM L-glutamine, and 20 μM CSIC-E379 when indicated, and cells were incubated at 37°C in a CO_2 -free incubator for 1 hr. Cells were then placed in the instrument, and basal oxygen consumption was recorded for 24 min. At the end of the run, 1 μM rotenone and 1 μM antimycin A were added to determine the mitochondria-independent oxygen consumption. Cells were lysed in 50 mM Tris, 150 mM NaCl, 2 mM EDTA, 1% NP40, 0.1% SDS, and 1% deoxycholate (pH 7.5), and the protein concentration was determined with the BCA method.

Cell Viability and Apoptosis Assays

Cell viability was evaluated with the Cell Proliferation Reagent WST-1 (Roche Diagnostics GmbH, Mannheim, Germany) following the manufacturer's instructions. For cell viability assays, 7000 cells were plated in 96-well plates and grown for 24 or 48 hr in the absence of serum and in the presence of the drugs. Ten microliters of WST-1 reagent was added to each well, cells were incubated for 4 hr, and the dye absorbance at 480 nm was measured using a Varioskan Flash (Thermo Fisher Scientific) plate reader. The absorbance at 690 nm was used as background.

Apoptosis was measured using Annexin-V and PI staining using the Vybrant Apoptosis Assay Kit (Invitrogen) and following the manufacturer's instructions; 300,000 cells were plated in 6-well plates and exposed to the different agents in absence of serum for 48 hr. Floating and adherent cells were collected and stained for 15 min at room temperature in the dark and were fluorescence analyzed using an EPICS XL flow cytometer.

Measurement of ROS

ROS levels were determined by incubating the cells with 2',7'-dichloro-dihydro-fluorescein diacetate (H_2 -DCFDA, Molecular Probes). A total of 300,000 cells were plated in 6-well plates and exposed to the different agents in absence of serum for 24 hr. Cells were incubated in the presence of 5 μM H_2 -DCFDA for 1 hr at 37°C and a humidified 5% CO_2 atmosphere in the dark. Floating and adherent cells were harvested in the same medium, and

the fluorescence was analyzed using an EPICS XL flow cytometer. Cells treated for 1 hr with 10 μ M rotenone were used as control.

Statistical Analysis

All values are expressed as mean \pm SEM of at least three independent experiments performed in triplicate. Differences between groups were determined using either two-tailed unpaired Student's *t* tests or the one-way ANOVA test using the SigmaPlot software. Significant differences between groups are indicated as **p* < 0.05, ***p* < 0.01, and ****p* < 0.001.

SUPPLEMENTAL INFORMATION

Supplemental Information includes Supplemental Experimental Procedures and four figures and can be found with this article online at [doi:10.1016/j.chembiol.2010.12.012](https://doi.org/10.1016/j.chembiol.2010.12.012).

ACKNOWLEDGMENTS

This work was supported by project grants of the Spanish Ministry of Science and Innovation (SAF2009-07126, Consolider-Ingenio 2010 CSD2007-00020, and CTQ 2009-07752), CSIC (2004 2 OE 238), and Comunidad de Madrid (S-SAL-0249-2006). We also thank the Ministry of Education for a doctoral fellowship to E.C. M.M.G.B. was supported by the "Ramón y Cajal" program. The expert technical assistance of Pilar Zaragoza is gratefully acknowledged.

Received: July 30, 2010

Revised: November 15, 2010

Accepted: December 6, 2010

Published: February 24, 2011

REFERENCES

- Altucci, L., Leibowitz, M.D., Ogilvie, K.M., de Lera, A.R., and Gronemeyer, H. (2007). RAR and RXR modulation in cancer and metabolic disease. *Nat. Rev. Drug Discov.* 6, 793–810.
- Alvarez, R., de Andrés, J., Yubero, P., Viñas, O., Mampel, T., Iglesias, R., Giral, M., and Villarroja, F. (1995). A novel regulatory pathway of brown fat thermogenesis: retinoic acid is a transcriptional activator of the mitochondrial uncoupling protein gene. *J. Biol. Chem.* 270, 5666–5673.
- Arechaga, I., Raimbault, S., Prieto, S., Levi-Meyrueis, C., Zaragoza, P., Miroux, B., Ricquier, D., Bouillaud, F., and Rial, E. (1993). Cysteine residues are not essential for uncoupling protein function. *Biochem. J.* 296, 693–700.
- Azzu, V., and Brand, M.D. (2010). The on-off switches of the mitochondrial uncoupling proteins. *Trends Biochem. Sci.* 35, 298–307.
- Baffy, G. (2010). Uncoupling protein-2 and cancer. *Mitochondrion* 10, 243–252.
- Bernard, A.M., Cocco, M.T., Onnis, V., and Piras, P.P. (1998). Facile synthesis of 2,2-dimethylchromans by Mo(CO)₆ catalyzed reaction of aryl prenyl ethers. *Synthesis* 3, 256–258.
- Bouillaud, F. (2009). UCP2, not a physiologically relevant uncoupler but a glucose sparing switch impacting ROS production and glucose sensing. *Biochim. Biophys. Acta* 1787, 377–383.
- Brand, M.D., and Esteves, T.C. (2005). Physiological functions of the mitochondrial uncoupling proteins UCP2 and UCP3. *Cell Metab.* 2, 85–93.
- Brand, M.D., Pakay, J.L., Ocloo, A., Kokoszka, J., Wallace, D.C., Brookes, P.S., and Cornwall, E.J. (2005). The basal proton conductance of mitochondria depends on adenine nucleotide translocase content. *Biochem. J.* 392, 353–362.
- Burnel, R.H., and Caron, S. (1992). Approach to the synthesis of candelabrone and synthesis of 3,7-diketo-12-hydroxyabieta-8,11,13-triene. *Can. J. Chem.* 70, 1446–1454.
- Cannon, B., Shabalina, I.G., Kramarova, T.V., Petrovic, N., and Nedergaard, J. (2006). Uncoupling proteins: a role in protection against reactive oxygen species—or not? *Biochim. Biophys. Acta* 1757, 449–458.
- Carretero, M.V., Torres, L., Latasa, U., García-Trevijano, E.R., Prieto, J., Mato, J.M., and Avila, M.A. (1998). Transformed but not normal hepatocytes express UCP2. *FEBS Lett.* 439, 55–58.
- Couplan, E., Gonzalez-Barroso, M.M., Alves-Guerra, M.C., Ricquier, D., Goubern, M., and Bouillaud, F. (2002). No evidence for a basal, retinoic, or superoxide-induced uncoupling activity of the uncoupling protein 2 present in spleen or lung mitochondria. *J. Biol. Chem.* 277, 26268–26275.
- Derdak, Z., Mark, N.M., Beldi, G., Robson, S.C., Wands, J.R., and Baffy, G. (2008). The mitochondrial uncoupling protein-2 promotes chemoresistance in cancer cells. *Cancer Res.* 68, 2813–2819.
- Echtay, K.S. (2007). Mitochondrial uncoupling proteins—what is their physiological role? *Free Radic. Biol. Med.* 43, 1351–1371.
- Echtay, K.S., Roussel, D., St-Pierre, J., Jekabsons, M.B., Cadenas, S., Stuart, J.A., Harper, J.A., Roebuck, S.J., Morrison, A., Pickering, S., et al. (2002). Superoxide activates mitochondrial uncoupling proteins. *Nature* 415, 96–99.
- Echtay, K.S., Esteves, T.C., Pakay, J.L., Jekabsons, M.B., Lambert, A.J., Portero-Otín, M., Pamplona, R., Vidal-Puig, A.J., Wang, S., Roebuck, S.J., and Brand, M.D. (2003). A signalling role for 4-hydroxy-2-nonenal in regulation of mitochondrial uncoupling. *EMBO J.* 22, 4103–4110.
- González-Barroso, M.M., Fleury, C., Bouillaud, F., Nicholls, D.G., and Rial, E. (1998). The uncoupling protein UCP1 does not increase the proton conductance of the inner mitochondrial membrane by functioning as a fatty acid anion transporter. *J. Biol. Chem.* 273, 15528–15532.
- González-Barroso, M.M., Fleury, C., Jiménez, M.A., Sanz, J.M., Romero, A., Bouillaud, F., and Rial, E. (1999). Structural and functional study of a conserved region in the uncoupling protein UCP1: the three matrix loops are involved in the control of transport. *J. Mol. Biol.* 292, 137–149.
- Harper, M.E., Antoniou, A., Villalobos-Menuet, E., Russo, A., Trauger, R., Vendemio, M., George, A., Bartholomew, R., Carlo, D., Shaikh, A., et al. (2002). Characterization of a novel metabolic strategy used by drug-resistant tumor cells. *FASEB J.* 16, 1550–1557.
- Hatakeyama, Y., and Scarpace, P.J. (2001). Transcriptional regulation of uncoupling protein-2 gene expression in L6 myotubes. *Int. J. Obes. Relat. Metab. Disord.* 25, 1619–1624.
- Heaton, G.M., and Nicholls, D.G. (1976). The calcium conductance of the inner membrane and the determination of the calcium electrochemical gradient. *Biochem. J.* 156, 635–646.
- Horimoto, M., Resnick, M.B., Konkin, T.A., Routhier, J., Wands, J.R., and Baffy, G. (2004). Expression of uncoupling protein-2 in human colon cancer. *Clin. Cancer Res.* 10, 6203–6207.
- Ishino, Y., Mihara, M., Hayakawa, N., Miyata, T., Kaneko, Y., and Miyata, T. (2001). An improved method for synthesis of 1-benzopyrans from unsaturated alcohols and phenols using a catalytic amount of acids. *Synth. Commun.* 31, 439–448.
- Janusz, J.M., Young, P.A., Scherz, M.W., Enzweiler, K., Wu, L.I., Gan, L., Pikul, S., McDow-Dunham, K.L., Johnson, C.R., Senanayake, C.B., et al. (1998). New cyclooxygenase-2/5-lipoxygenase inhibitors. 2. 7-tert-Butyl-2,3-dihydro-3,3-dimethylbenzofuran derivatives as gastrointestinal safe antiinflammatory and analgesic agents: variations of the dihydrobenzofuran ring. *J. Med. Chem.* 41, 1124–1137.
- Jiménez-Jiménez, J., Zardoya, R., Ledesma, A., García de Lacoba, M., Zaragoza, P., González-Barroso, M.M., and Rial, E. (2006). Evolutionarily distinct residues in the uncoupling protein UCP1 are essential for its characteristic basal proton conductance. *J. Mol. Biol.* 359, 1010–1022.
- Khailova, L.S., Prihodko, E.A., Dedukhova, V.I., Mokhova, E.N., Popov, V.N., and Skulachev, V.P. (2006). Participation of ATP/ADP antiporter in oleate- and oleate hydroperoxide-induced uncoupling suppressed by GDP and carboxyatractylate. *Biochim. Biophys. Acta* 1757, 1324–1329.
- Kim, S.J., Kim, J.K., Lee, D.U., Kwak, J.H., and Lee, S.M. (2010). Genipin protects lipopolysaccharide-induced apoptotic liver damage in D-galactosamine-sensitized mice. *Eur. J. Pharmacol.* 635, 188–193.
- Koo, H.J., Song, Y.S., Kim, H.J., and Park, E.H. (2004). Antiinflammatory effects of genipin, an active principle of gardenia. *Eur. J. Pharmacol.* 495, 201–208.

- Krauss, S., Zhang, Z.Y., and Lowell, B.B. (2005). The mitochondrial uncoupling-protein homologues. *Nat. Rev. Mol. Cell Biol.* 6, 248–261.
- Lau, A.T., Wang, Y., and Chiu, J.F. (2008). Reactive oxygen species: current knowledge and applications in cancer research and therapeutic. *J. Cell. Biochem.* 104, 657–667.
- Ledesma, A., García de Lacoba, M., and Rial, E. (2002a). The mitochondrial uncoupling proteins. *Genome Biol.* 3, 3015.1–3015.9.
- Ledesma, A., García de Lacoba, M., Arechaga, I., and Rial, E. (2002b). Modeling the transmembrane arrangement of the uncoupling protein UCP1 and topological considerations of the nucleotide-binding site. *J. Bioenerg. Biomembr.* 34, 473–486.
- Mailloux, R.J., Adjeitey, C.N., and Harper, M.E. (2010). Genipin-induced inhibition of uncoupling protein-2 sensitizes drug-resistant cancer cells to cytotoxic agents. *PLoS ONE* 5, e13289.
- McKean, D.R., Parrinello, G., Renaldo, A.F., and Stille, J.K. (1987). Synthesis of functionalized styrenes via palladium-catalyzed coupling of aryl bromides with vinyl tin reagents. *J. Org. Chem.* 52, 422–424.
- Nübel, T., and Ricquier, D. (2006). Respiration under control of UCPs: clinical perspective. *Horm. Res.* 65, 300–310.
- Nury, H., Dahout-Gonzalez, C., Trézéguet, V., Lauquin, G.J., Brandolin, G., and Pebay-Peyroula, E. (2006). Relations between structure and function of the mitochondrial ADP/ATP carrier. *Annu. Rev. Biochem.* 75, 713–741.
- Pani, G., Galeotti, T., and Chiarugi, P. (2010). Metastasis: cancer cell's escape from oxidative stress. *Cancer Metastasis Rev.* 29, 351–378.
- Rial, E., and González-Barroso, M.M. (2001). Physiological regulation of the transport activity in the uncoupling proteins UCP1 and UCP2. *Biochim. Biophys. Acta* 1504, 70–81.
- Rial, E., González-Barroso, M.M., Fleury, C., Iturrizaga, S., Sanchis, D., Jiménez-Jiménez, J., Ricquier, D., Goubert, M., and Bouillaud, F. (1999). Retinoids activate proton transport by the uncoupling proteins UCP1 and UCP2. *EMBO J.* 18, 5827–5833.
- Rial, E., Rodríguez-Sánchez, L., Gallardo-Vara, E., Zaragoza, P., Moyano, E., and González-Barroso, M.M. (2010). Lipotoxicity, fatty acid uncoupling and mitochondrial carrier function. *Biochim. Biophys. Acta* 1797, 800–806.
- Samudio, I., Fiegl, M., McQueen, T., Clise-Dwyer, K., and Andreeff, M. (2008). The warburg effect in leukemia-stroma cocultures is mediated by mitochondrial uncoupling associated with uncoupling protein 2 activation. *Cancer Res.* 68, 5198–5205.
- Sánchez, Y., Amrán, D., Fernández, C., de Blas, E., and Aller, P. (2008). Genistein selectively potentiates arsenic trioxide-induced apoptosis in human leukemia cells via reactive oxygen species generation and activation of reactive oxygen species-inducible protein kinases (p38-MAPK, AMPK). *Int. J. Cancer* 123, 1205–1214.
- Santandreu, F.M., Valle, A., Fernández de Mattos, S., Roca, P., and Oliver, J. (2009). Hydrogen peroxide regulates the mitochondrial content of uncoupling protein 5 in colon cancer cells. *Cell. Physiol. Biochem.* 24, 379–390.
- Santandreu, F.M., Roca, P., and Oliver, J. (2010). Uncoupling protein-2 knock-down mediates the cytotoxic effects of cisplatin. *Free Radic. Biol. Med.* 49, 658–666.
- Sastre-Serra, J., Valle, A., Company, M.M., Garau, I., Oliver, J., and Roca, P. (2010). Estrogen down-regulates uncoupling proteins and increases oxidative stress in breast cancer. *Free Radic. Biol. Med.* 48, 506–512.
- Shabalina, I.G., Hoeks, J., Kramarova, T.V., Schrauwen, P., Cannon, B., and Nedergaard, J. (2010). Cold tolerance of UCP1-ablated mice: a skeletal muscle mitochondria switch toward lipid oxidation with marked UCP3 up-regulation not associated with increased basal, fatty acid- or ROS-induced uncoupling or enhanced GDP effects. *Biochim. Biophys. Acta* 1797, 968–980.
- Slusarewicz, P., Zhu, K., and Hedman, T. (2010). Kinetic characterization and comparison of various protein crosslinking reagents for matrix modification. *J. Mater. Sci. Mater. Med.* 21, 1175–1181.
- Swida-Barteczka, A., Woyda-Ploszczyca, A., Sluse, F.E., and Jarmuszkiewicz, W. (2009). Uncoupling protein 1 inhibition by purine nucleotides is under the control of the endogenous ubiquinone redox state. *Biochem. J.* 424, 297–306.
- Teng, M., Duong, T.T., Johnson, A.T., Klein, E.S., Wang, L., Khalifa, B., and Chandraratna, R.A.S. (1997). Identification of highly potent retinoic acid receptor α -selective antagonists. *J. Med. Chem.* 40, 2445–2451.
- Tomás, P., Jiménez-Jiménez, J., Zaragoza, P., Vuligonda, V., Chandraratna, R.A.S., and Rial, E. (2004). Activation by retinoids of the uncoupling protein UCP1. *Biochim. Biophys. Acta* 1658, 157–164.
- Tomás, P., Ledesma, A., and Rial, E. (2002). Photoaffinity labeling of the uncoupling protein UCP1 with retinoic acid: ubiquinone favors binding. *FEBS Lett.* 526, 63–65.
- Trachootham, D., Alexandre, J., and Huang, P. (2009). Targeting cancer cells by ROS-mediated mechanisms: a radical therapeutic approach? *Nat. Rev. Drug Discov.* 8, 579–591.
- Yamazaki, M., and Chiba, K. (2008). Genipin exhibits neurotrophic effects through a common signaling pathway in nitric oxide synthase-expressing cells. *Eur. J. Pharmacol.* 581, 255–261.
- Yi, J., Gao, F., Shi, G., Li, H., Wang, Z., Shi, X., and Tang, X. (2002). The inherent cellular level of reactive oxygen species: one of the mechanisms determining apoptotic susceptibility of leukemic cells to arsenic trioxide. *Apoptosis* 7, 209–215.
- Zhang, C.Y., Parton, L.E., Ye, C.P., Krauss, S., Shen, R., Lin, C.T., Porco, J.A., Jr., and Lowell, B.B. (2006). Genipin inhibits UCP2-mediated proton leak and acutely reverses obesity- and high glucose-induced beta cell dysfunction in isolated pancreatic islets. *Cell Metab.* 3, 417–427.
- Zhou, H., Zhao, J., and Zhang, X. (2009). Inhibition of uncoupling protein 2 by genipin reduces insulin-stimulated glucose uptake in 3T3-L1 adipocytes. *Arch. Biochem. Biophys.* 486, 88–93.